Journal of Bio- and Tribo-Corrosion (2018) 4:63
https://doi.org/10.1007/s40735-018-0180-x

Anticorrosion Performance of *Mitracarpus hirtus* Extract on Mild Steel in 1 M HCl

R. Ragul[1] · S. Kathiravan[1] · A. Murugesh[1] · J. Ravichandran[1]

Received: 25 June 2018 / Revised: 2 August 2018 / Accepted: 27 August 2018 / Published online: 4 September 2018

Abstract
The methanol extract of *Mitracarpus hirtus* leaves (MMH) as a corrosion inhibitor for mild steel (MS) in 1 M HCl was probed by weight loss, colorimetric, and electrochemical methods, varying the concentrations of the inhibitor, acid, added halide ions, and temperature. The maximum efficiency of 89.06% was obtained at an inhibitor concentration of 0.6 g/L. The results suggest that the percentage of inhibition efficiency increases with an increase in MMH concentration and decreases with temperature. Thermodynamic parameters indicate the spontaneous adsorption of MMH on MS surface. It has been confirmed by Langmuir adsorption process. The chemical constituents for MMH adsorption on MS surface were confirmed by Fourier transform infrared spectroscopy, field emission scanning electron microscopy, and energy dispersive X-ray spectrometer.

Keywords Mild steel · Weight loss · Colorimetric · Electrochemical · FT-IR · FESEM-EDS

1 Introduction

Mild steel because of its low cost and good mechanical strength is used in a variety of industries like automobile, construction, chemical etc. Mild steel is affected by corrosion to a different extent in different industries due to the nature of the environment [1, 2]. Acid solutions are used in pickling, descaling, oil well acidizing etc. [3, 4]. Mostly acid pickling baths containing hydrochloric acid are widely used in industrial cleaning. Hydrochloric acid is highly corrosive to mild steel. The use of inhibitor is one of the most practical methods for corrosion protection. The addition of the inhibitor reduces the chemical attack on mild steel. Organic inhibitors are a mixture of compounds containing nitrogen, sulphur, oxygen atoms as well as multiple bonds in their molecule. Volumes of literature are available regarding the use of synthetic compounds as a corrosion inhibitor for various metals [5–13]. However, the use of synthetic inhibitor is limited due to their high cost and hazardous nature. Recently, researchers have turned their attention on green inhibitors because they are biodegradable, inexpensive, and readily available in nature [14, 15]. Further, the plant extracts are present in the bioactive compounds are very efficient like synthetic inhibitors [16, 17]. *Thymelaea hirsuta* [18], *Psidium guajava* [19], *Cassia auriculata* [20], *Luffa aegyptiaca* [21], *Clematis gouriana* [22], *Phyllanthus amarus* [23], *Uncaria gambir* [24], *Murraya koenigii* [25], *Schinopsis lorentzii* [26], *Brugmansia suaveolens* [27], *Ruellia tuberosa* [28], *Desmodium triflorum and Zanthoxylum alatum* [29, 30] are some of the recently reported green inhibitors.

Mitracarpus hirtus (MH) belonging to the family of Rubiaceae, which is a weed, grows on its own. This plant is used in local medicine for the treatment of skin diseases. It is found to contain phytochemical constituents like alkaloids, flavonoids, terpenoids, saponins, tannins, etc. [31]. However, there are no reports on the use of the extracts of this plant in corrosion inhibition studies. Hence, in the present work, an attempt has been made to probe the inhibitive action of methanol extract of MH on mild steel corrosion in HCl medium. Confirmation of MMH as corrosion inhibitor was done through weight loss, colorimetric, AC impedance spectroscopy and potentiodynamic polarization spectroscopy. The protective film found on metal surface was characterized by analytical techniques like Fourier transform infrared spectroscopy (FT-IR), field emission scanning electron microscope (FESEM) and energy-dispersive X-ray spectrometer (EDS).

✉ J. Ravichandran
jrsrmvchem@gmail.com

[1] Postgraduate and Research Department of Chemistry, Sri Ramakrishna Mission Vidyalaya College of Arts and Science, Coimbatore, Tamil Nadu 641020, India

2 Experimental Details

2.1 Specimen Preparation

The mild steel specimen of dimensions $1.039 \times 5.15 \times 0.293$ cm with an area of 14.3284 cm^2 was used for the weight loss method. The specimen surface was mechanically polished with different grade emery papers (400, 600, 1000 and 1500), cleaned with acetone and stored in a desiccator. The chemical composition of MS used is as follows: C—0.088%, Mn—0.540%, P—0.012%, Cr—0.013%, Si—0.014%, Cu—0.016%, S—0.012%, Ni—0.021%, Mo—0.002%, Al—0.059%, V—0.001%, W—0.01 and the rest is Fe.

2.2 Preparation of the Extract

Mitracarpus hirtus plant was collected from the Nilgiris, Tamil Nadu, South India. The leaves were air dried for 15 days in the shade and ground into powder. 20 g of the powdered leaves was extracted in soxhlet apparatus with 175 mL methanol for 9 h at 60 °C. Thereafter, the solution was evaporated to about 50 mL on a water bath. The concentrated extract was dried to complete dryness. A stock solution was prepared by dissolving 1 g of the dried sample in 500 mL of methanol. Desired concentrations of the methanol extract of leaves (MMH) namely 0.1–0.6 g/L were obtained by properly diluting the stock solution to make 100 mL of the test solution. The test solution was freshly prepared before each experiment.

2.3 Weight Loss Method

Weight loss method is one of the oldest and simplest methods for monitoring corrosion. Hence, weight loss method has been used as one of the methods in the present study to evaluate the performance of the inhibitor. Here, the MS specimens were polished following the standard procedure [32] and stored in a desiccator. The polished specimen in triplicate was weighed and immersed in 100 mL of 1 M hydrochloric acid solution without and with different concentrations of inhibitors (0.1–0.6 g/L) for the immersion periods of 1–5 h. Later, the specimens were removed from the test solutions, washed with distilled water, dried and reweighed. The inhibition efficiency was calculated from the weight loss data and the optimum concentration of the inhibitor was found out. The concentration of acid was increased from 1 to 4 M in order to find the effectiveness of inhibitor at high concentration range. Halide additives were added to study synergistic their influence on inhibition efficiency of the inhibitor. To assertion, the influence of temperature on the performance of the inhibitor, corrosion behaviour of MS in the presence of MMH was also studied by varying the temperature from 303 to 333 K. The percentage inhibition efficiency (%IE) was determined, using the following equation:

$$\%\mathrm{IE} = [(W_\mathrm{b} - W_i)/W_\mathrm{b}] \times 100, \tag{1}$$

where W_b and W_i are the weight loss of the MS specimens in the absence of inhibitor and in the presence of inhibitor, respectively. The corrosion rate (CR) was calculated by the following equation:

$$\mathrm{CR} = \frac{K\Delta W}{\rho A t} \tag{2}$$

$K = 3.45 \times 10^6$ to given CR in mpy, where W is the weight loss (mg); ρ is the density of the specimen (g cm^{-3}); A is the area of the specimen (cm^2), and t is the exposure time (h).

To evaluate the performance of the inhibitor using additional methods like colorimetric and electrochemical studies. The weight loss study we have used the same solution after immersion studies for colourimetric studies to quantify the amount of iron in the solution and hence the % of inhibition efficiency. Potentiodynamic polarization studies and electrochemical impedance spectroscopy studies are proven technique to quickly evaluate the performance of the inhibitor.

2.4 Colorimetric Estimation

The amount of iron present in the corrosive medium after immersion studies can give us an indication of the extent of corrosion. Hence to determine the amount of iron in the test solution, colorimetric experiments were carried out varying the concentration of inhibitor and time of immersion. The colouring agent is phenanthroline, hydroxylamine hydrochloride, and buffer solutions were mixed to the standard ferrous ammonium sulphate solutions to produces colours of varying intensities. The absorbances of these solutions were measured using the Baush & Lomb spectronic 20 colorimeter. A standard graph was plotted taking absorbance in y-axis and concentration of iron (10^{-3} g) in x-axis. The absorbance of the inhibited and uninhibited solutions after immersion experiments was found out and from the standard graph, the amount of iron present the solution was found out and % inhibition efficiency was calculated using the equation given below:

$$\%\mathrm{IE} = [(C - C^\mathrm{o})/C] \times 100, \tag{3}$$

where C is a concentration of Fe^{2+} in uninhibited solution; C^o is a concentration of Fe^{2+} in inhibited solution.

2.5 Electrochemical Methods

Electrochemical impedance spectroscopy (EIS) and potentiodynamic polarization (PDP) studies were carried out using electrochemical analyser of CH Instrument (model 608D) in a three-electrode cell assembly. Platinum was used as a counter electrode and calomel as the reference electrode. MS specimen having an exposed area of 0.95 cm^2 was used as working electrode. The volume of the test solution was maintained at 100 mL for all electrochemical experiments. Before each experiment, the MS specimens were polished employing the standard procedure described elsewhere [33]. EIS measurements were made in the frequency range of 10 kHz–1 Hz at the rest of potential using 0.02 V peak to peak with the alternating current signal. The impedance data were obtained from the Nyquist plots. The %IE was calculated from the given equation:

$$\%IE = ((R_{ct} - R_{ct(b)})/R_{ct}) \times 100, \quad (4)$$

where R_{ct} and $R_{ct(b)}$ are the charge transfer resistance values in the presence and absence of inhibitor, respectively. PDP studies were carried out at a scan rate of 0.01 V/s in the potential range from −0.75 to −0.25 V. The corrosion current density values (I_{corr}) were obtained from the Tafel plots. The %IE was calculated from the following equation:

$$\%IE = ((I_{corr(b)} - I_{corr(i)})/ I_{corr(b)}) \times 100, \quad (5)$$

where $I_{corr(b)}$ and $I_{corr(i)}$ are the values of corrosion current densities in the absence and presence of inhibitor, respectively.

2.6 FESEM and EDS Analysis

Surface morphology of the MS for fresh inhibited and uninhibited specimens was also examined using field emission scanning electron microscope (FESEM) coupled with energy dispersive X-ray spectroscopy (EDS).

2.7 FT-IR Spectral Analysis

The FT-IR spectra of MMH residue and the scrapped material from mild steel surface obtained after immersion studies were recorded using KBr pellet technique.

3 Results and Discussion

3.1 Weight Loss Method

The corrosion rate and inhibition efficiency values obtained using weight loss studies are given in Table 1. It shows the effect of the inhibitor concentration (0.1–0.6 g/L) on the corrosion of mild steel in 1 M HCl at different immersion periods (1–5 h). The maximum efficiency was obtained at an inhibitor concentration of 0.6 g/L with an immersion time of 3 h. The increase in %IE with the inhibitor concentration indicates that the inhibitor molecules adsorbed on the metal surface. Similarly, the decrease in %IE after an immersion period of 3 h indicates the desorption of the inhibitor molecules from the metal surface.

The data on the corrosion of MS at different concentrations of acid are shown in Table 2. The results indicate that the %IE decreases and the corrosion rate increases at higher concentrations of the acid. This might be due to the fact that at higher concentrations of the acid the rate of chemical reaction is increased and this controls the adsorption power of the inhibitor, molecules by the ionization of active species associated into the inhibitor [34]. At higher acid concentrations, the acid may also form a metal-hydrogen bond by ruptured of the metal surface leading to the decrease in surface coverage by the inhibitor molecules.

The results of the influence of halide ions on the inhibition efficiency of the inhibitor MMH were studied by adding 10^{-3} g/L of KI and KBr to the test solutions with and

Table 1 Influence of concentration of MMH on the corrosion of MS in 1 M HCl at different immersion periods

S. no.	MMH conc. (g/L)	Immersion time					
		1 h		3 h		5 h	
		CR (mpy)	IE (%)	CR (mpy)	IE (%)	CR (mpy)	IE (%)
1	Blank	1558	–	1112	–	1009	–
2	0.1	980	37.11	582	47.67	480	52.12
3	0.2	648	58.39	323	70.92	334	66.84
4	0.3	462	70.31	258	76.75	231	77.03
5	0.4	328	78.91	184	83.40	168	83.30
6	0.5	216	86.13	117	89.42	144	88.66
7	0.6	170	89.06	104	90.61	114	88.72

Table 2 Effect of concentration of HCl on the corrosion of MS with MMH

S. no.	MMH conc. (g/L)	HCl concentration							
		1 M		2 M		3 M		4 M	
		CR (mpy)	IE (%)	CR (mpy)	IE (%)	CR (mpy)	IE (%)	CR (mpy)	IE (%)
1	Blank	1558	–	1716	–	1975	–	2373	–
2	0.1	980	37.11	1384	19.32	1634	17.25	2145	9.61
3	0.2	648	58.39	1031	39.82	1558	21.10	2072	12.69
4	0.3	462	70.31	846	50.70	1269	35.75	1832	22.82
5	0.4	328	78.91	703	59.04	1025	48.07	1655	30.25
6	0.5	216	86.13	499	70.92	836	57.62	1390	41.41
7	0.6	170	89.06	337	80.31	693	64.87	1235	47.94

Table 3 Effect of addition of halide additives on the corrosion inhibition of MS by MMH in 1 M HCl at 1-h immersion time

S. no.	MMH conc. (g/L)	Added halide additives			
		With KBr		With KI	
		CR (mpy)	IE (%)	CR (mpy)	IE (%)
1	Blank	1558	–	1549	–
2	0.1	736	52.73	700	54.81
3	0.4	152	90.23	164	89.39
4	0.6	100	93.55	127	91.74

without inhibitor and the results are presented in Table 3. The influence of halide ions on the inhibition efficiency of various synthetic and natural inhibitors has been reported by many authors [35–38]. Reports suggested both synergistic and antagonistic effects depending on the reaction system under study. The above results clearly show that addition of KBr produces synergistic influence indicating a bridge between the metal atom and the inhibitor. However, the addition of KI produces antagonistic effect suggesting a weaker interaction between the halide ions (KI) and the inhibitor molecules [39].

To study the influence of temperature on the methanol extract of MH on mild steel corrosion in 1 M HCl, experiments were carried out in the temperature range of 303–333 K. The results are present in Table 4. The results vividly indicate that when the temperature is increased from 303 to 333 K the inhibition efficiency decreased from 92.01 to 75.33%. Generally, the adsorption and desorption of inhibitor molecules take place continuously on the metal surface. At higher temperatures, due to the higher dissolution of metal, the rate of desorption overcomes the rate of adsorption. This is also supportive of the fact that the adsorption is physical in nature. The adsorbed layer is desorbed early at higher temperature [40–42].

3.2 Colorimetric Estimation

In the colorimetric analysis, the amount of iron present in inhibited and uninhibited test solutions was quantified using a colorimeter. Colorimetric experiments were carried out after immersion experiments on all the test solutions used in gravimetric studies. The results are given in Table 5, and it reveals that with the increase in the concentration of inhibitor, the iron content of the solution decreases suggesting the decrease in CR which in turn indicates the increase in %IE. The corresponding %IE values obtained from these data also increase up to the optimum concentrations of MMH. The immersion time is another important parameter which ascertains the inhibitive effect of the inhibitor on standing. In the present study, the effect of immersion time (1–5 h) on corrosion inhibition

Table 4 Influence of temperature on the corrosion inhibition of MS in 1 M HCl with different concentrations of MMH at 1-h immersion time

S. no.	MMH conc. (g/L)	303 K		313 K		323 K		333 K	
		CR (mpy)	IE (%)	CR (mpy)	IE (%)	CR (mpy)	IE (%)	CR (mpy)	IE (%)
1	0	1637	–	2273	–	5152	–	7788	–
2	0.1	949	42.01	1460	35.74	3901	24.27	6230	20.00
3	0.2	526	67.84	1202	47.12	2994	41.87	4687	39.82
4	0.3	325	80.11	846	62.78	2069	59.83	3883	50.13
5	0.4	258	84.20	599	73.62	1433	72.17	3061	60.68
6	0.5	164	89.96	444	80.45	1031	79.97	2373	69.51
7	0.6	130	92.01	276	87.81	727	85.88	1886	75.77

Table 5 Colorimetric data for the corrosion inhibition of MS in 1 M HCl at various concentrations of MMH at room temperature

MMH Conc. (g/L)	1 h			3 h			5 h		
	Absorbance	Weight of iron 10^{-3} g	IE (%)	Absorbance	Weight of iron 10^{-3} g	IE (%)	Absorbance	Weight of iron 10^{-3} g	IE (%)
Blank	0.15	29.00	–	0.26	51.41	–	0.24	47.34	–
0.1	0.12	22.90	21.03	0.17	33.30	35.22	0.20	39.20	17.19
0.2	0.10	18.80	35.17	0.14	26.90	47.67	0.17	33.10	30.08
0.3	0.09	16.80	42.06	0.11	20.90	59.34	0.11	20.90	55.85
0.4	0.07	12.75	63.40	0.09	16.80	67.32	0.10	18.80	60.28
0.5	0.05	8.680	70.06	0.05	8.700	83.07	0.09	16.80	64.51
0.6	0.03	4.610	84.10	0.03	4.610	91.03	0.08	7.270	84.64

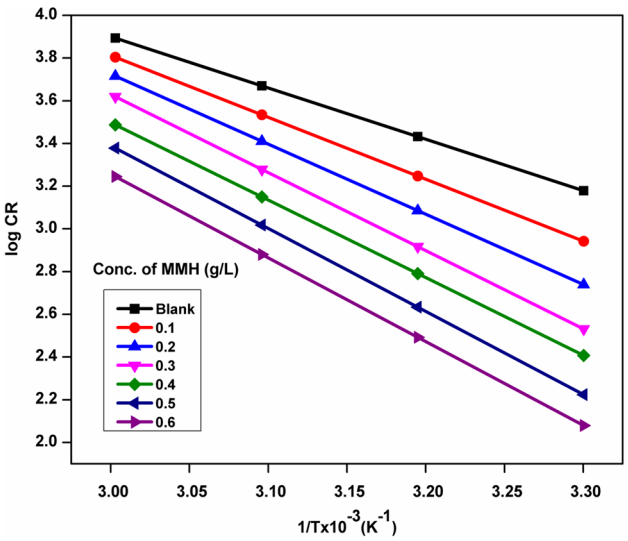

Fig. 1 Arrhenius plot (log CR vs 1/*T*) for MS corrosion in 1 M HCl in the presence and absence of MMH

of MMH in 1 M HCl at room temperature was investigated by colorimetric method. It is apparent from Table 5 that the %IE increases gradually with increasing immersion time and attains a maximum value of 91.03% with 0.6 g/L of MMH at an immersion period of 3 h. The inhibition efficiency increases from 1 to 3 h and beyond 3 h it starts declining. The increase in %IE with increasing immersion time is due to the increase in the surface coverage with time. However, the decrease in inhibition efficiency at higher immersion period might be due to the desorption of MMH on standing. The %IE values calculated from the colorimetric data are in good agreement with the data obtained from weight loss studies.

3.3 Thermodynamic Parameters

The energy of activation (E_a) was determined from the slope of the Arrhenius plot (log CR vs 1/*T*). In Fig. 1, the slope is equal to $E_a/2.303RT$. Here, CR is the corrosion rate. *T* is the temperature in absolute scale and *R* is the gas constant. The values along with other thermodynamic parameters are given in Table 6. It is clear from the table that the E_a values for the blank are less than that for the inhibited solutions. The higher values of E_a for the inhibited solutions are an indication of the fact that the inhibitor molecules are spontaneously adsorbed on the metal surface and the linkage between the metal and inhibitor is physical in nature [43]. The free energy of adsorption for different temperatures was calculated using the following Eq. (6).

$$\Delta G_{ads} = -RT \ln(55.5\ \text{K}), \tag{6}$$

Table 6 Values of activation energy and thermodynamic parameters for the corrosion inhibition of MS with and without different concentrations of MMH

S. no.	MMH conc. (g/L)	E_a (kJ mol^{-1})	$-\Delta G_{ads}$ (kJ mol^{-1})				$-\Delta H_{ads}$ (kJ mol^{-1})	ΔS_{ads} (kJ mol^{-1} K^{-1}) $\times 10^{-2}$
			303 K	313 K	323 K	333 K		
1	0	46.04	–	–	–	–	–	–
2	0.1	55.53	15.17	14.64	14.10	13.57	31.42	5.26
3	0.2	62.84	15.64	14.98	14.49	13.99	30.58	4.98
4	0.3	70.02	16.23	15.58	14.94	14.30	35.76	6.44
5	0.4	69.51	16.43	15.93	15.42	14.92	31.77	5.06
6	0.5	74.32	17.09	16.51	15.94	15.92	34.62	5.78
7	0.6	75.16	17.60	17.04	16.49	15.94	34.36	5.53

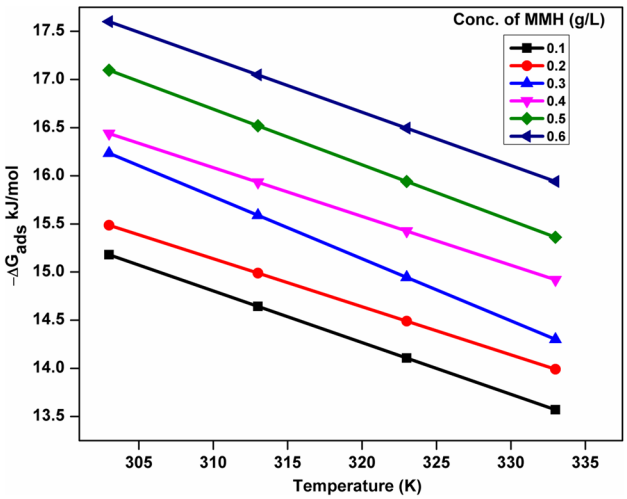

Fig. 2 ΔG_{ads} as a function of temperature in the presence of MMH in 1 M HCl

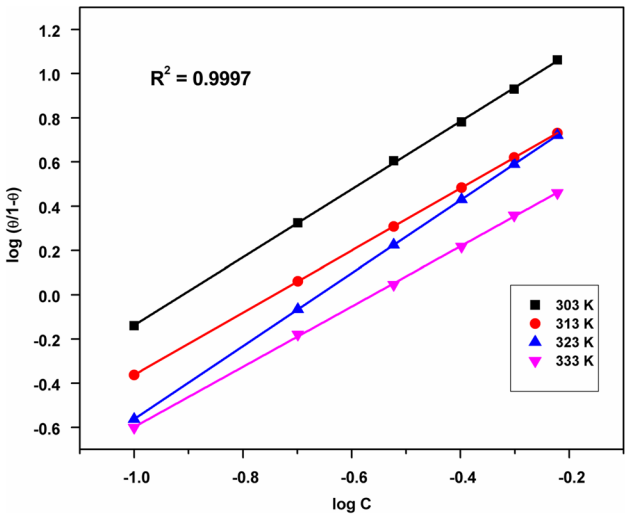

Fig. 3 Langmuir adsorption isotherm for MS corrosion in 1 M HCl in the presence of MMH

where 55.5—the number of moles of water per liter of solution, T—temperature in Kelvin scale, and K (equilibrium constant) $-\theta/C_{inh}(1-\theta)$. ΔH_{ads} and ΔS_{ads} values were obtained from the slope and intercept values ΔG_{ads} versus T plot (Fig. 2). The values of ΔG_{ads}, ΔH_{ads} and ΔS_{ads} are given in Table 6. The result presented in Table 6 indicates that the values of ΔG_{ads} are less negative than -20 kJ/mol suggesting that the process of inhibition is through physisorption. Further, the negative values of ΔG_{ads} point out the stability of the adsorption layer and the spontaneity of adsorption. Generally, negative values of ΔH_{ads} indicate an exothermic adsorption process. The ΔH_{ads} values are negative and ΔS_{ads} are positive. The negative value of ΔH_{ads} and the positive value of ΔS_{ads} particularize the feasibility of the reaction. Thus, the ΔG_{ads}, ΔH_{ads} and ΔS_{ads} values show that the process of adsorption of MMH is spontaneous and exothermic in nature.

3.4 Adsorption Isotherm

The nature of adsorption between the inhibitor molecules and the metal surface is well explained by adsorption isotherms. To find out the best-suited isotherm for the adsorption of MMH on MS surface, the surface coverage values obtained from weight loss data were fitted into various adsorption isotherms. Among the various isotherm tested, the Langmuir adsorption isotherm gave the best fit with correlation coefficient nearing almost unity. The Langmuir adsorption isotherm is represented by the equation.

$$\theta/(1-\theta) = K_{ads}C, \tag{7}$$

where K_{ads} is adsorption equilibrium constant and is related to the free energy of adsorption. The isotherm is obtained by plotting by log $(\theta/(1-\theta))$ versus log C as shown in Fig. 3. The straight lines with a correlation coefficient nearing unity confirm that adsorption of MMH on MS surface follows Langmuir isotherm.

3.5 Electrochemical Methods

3.5.1 AC Impedance Method

Impedance studies were carried out by varying the concentration of inhibitor (MMH) from 0.1 to 0.6 g/L. The Randles equivalent circuit used for impedance studies is

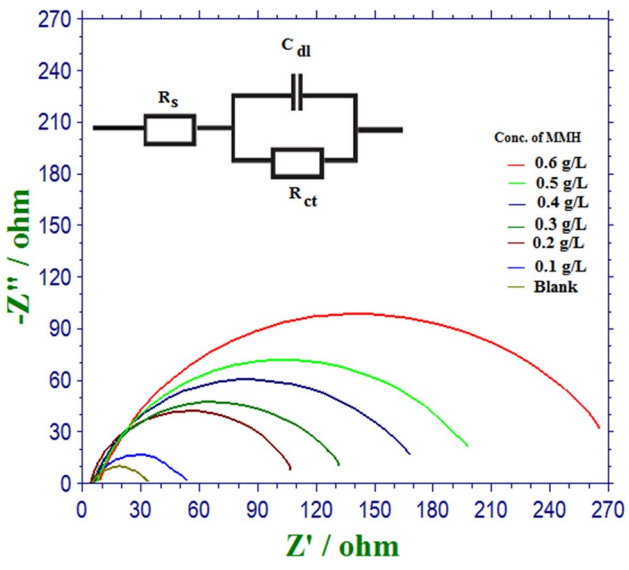

Fig. 4 Nyquist plots for the corrosion of MS in 1 M HCl with various concentrations of MMH

Table 7 Electrochemical parameters for MS corrosion in 1 M HCl at different concentrations of the inhibitor

MMH conc. (g/L)	PDP					EIS		
	b_a (mV dec^{-1})	b_c (mV dec^{-1})	$-E_{corr}$ (mV)	$I_{corr} \times 10^{-4}$ (Amp cm^{-2})	IE (%)	R_{ct} (Ω cm^2)	IE (%)	C_{dl} (F cm^{-2})
Blank	119.87	126.24	460.3	5.944	–	23.91	–	6.722
0.1	108.26	116.69	456.8	3.837	35.45	40.08	40.34	6.802
0.2	100.02	110.07	453.9	2.353	60.41	73.95	67.67	6.421
0.3	98.87	108.17	453.9	1.671	71.88	106.8	77.61	5.463
0.4	97.87	108.64	453.9	1.363	77.07	135	82.29	4.871
0.5	102.39	113.23	454.7	1.153	80.6	159	84.96	4.441
0.6	110.08	111.00	464.5	0.9433	84.13	213.7	88.81	3.908

given in Fig. 4, where R_s is solution resistance; C_{dl} is the double layer capacitance, and R_{ct} is the charge transfer resistance. The impedance data obtained from Nyquist plots are given in Table 7. The representative Nyquist plots for varying the concentration of inhibitor (MMH) are given in Fig. 4. The values of R_{ct} increased with increase in the concentration of inhibitors (MMH) and corresponding C_{dl} values decreased. The increasing R_{ct} value with an increase in inhibitor concentration is the result of an increase in the surface coverage by the inhibitor molecules. The decrease in C_{dl} value at higher the inhibitor concentration is due to increase in the thickness of the electrical double layer, indicating that the inhibitor is adsorbed on the metal surface. The diameter of impedance diagram increased on increasing the concentration of MMH indicating a strengthening of the inhibitive film at the metal surface. This is caused by the gradual replacement of water molecules by adsorption of inhibitor molecule on the iron surface [44–47].

3.5.2 Potentiodynamic Polarization Method

The electrochemical parameters such as corrosion potential (E_{corr}), corrosion current density (I_{corr}), cathodic slope (b_c) and anodic slope (b_a) were obtained from Tafel plots and inhibition efficiency (%IE) were calculated applying Eq. (5). Figure 5 depicts the representative Tafel plots of the corrosion inhibition studies on mild steel with different concentrations of MMH. The polarization data obtained are given in Table 7. The addition of inhibitor alters both b_a and b_c values suggesting that the inhibitor reduces both anodic dissolutions of the metal and retard hydrogen evolution reaction. This indicates the mixed nature of the inhibitor. The I_{corr} values decrease when increasing the concentration of inhibitors which are due to the higher surface coverage of the inhibitor [44–47].

3.6 FESEM and EDS Analysis

Surface morphology of MS was studied by field emission scanning electron microscopy after 3-h immersion in 1 M

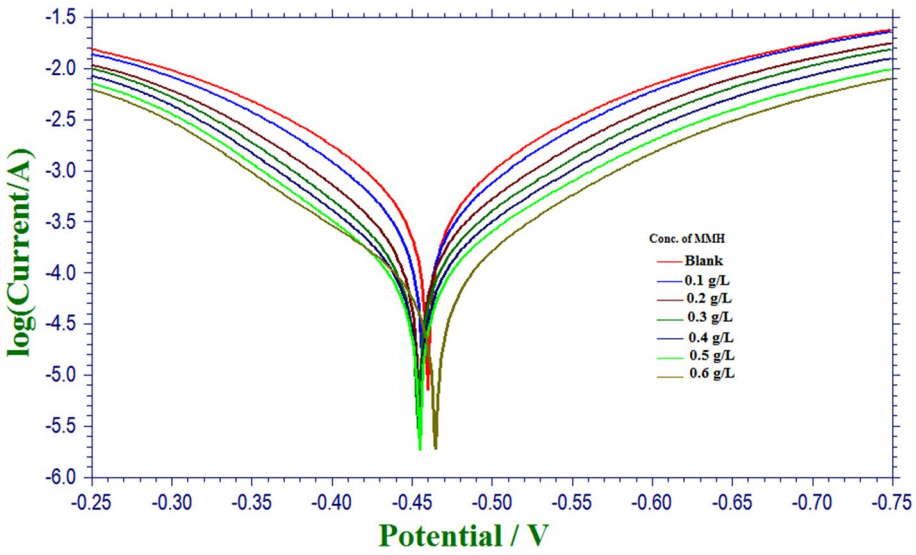

Fig. 5 Tafel plots for the corrosion of MS in the presence of various concentrations of MMH in 1 M HCl

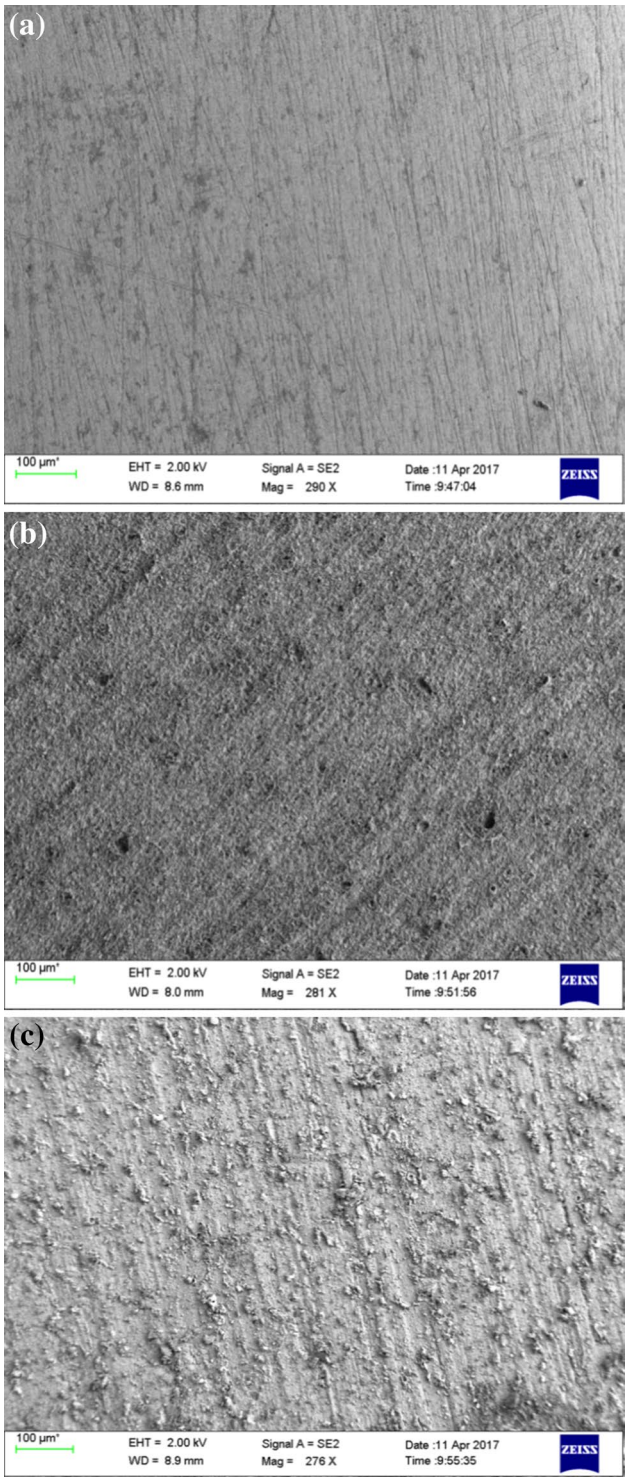

Fig. 6 SEM images of polished MS (**a**), MS in 1 M HCl (**b**), MS in 1 M HCl with MMH (**c**)

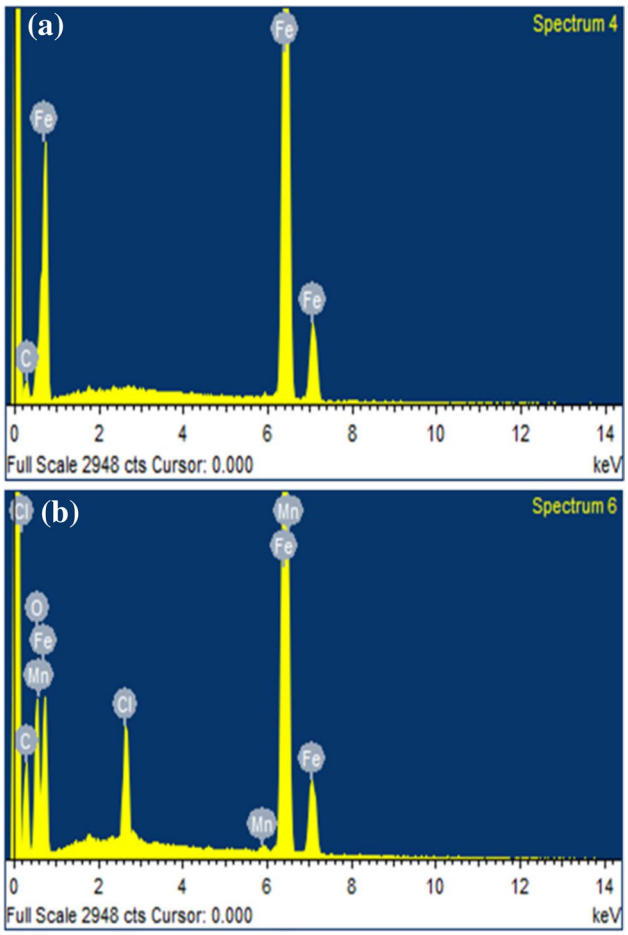

Fig. 7 EDS images **a** MS in 1 M HCl, **b** MS in 1 M HCl with MMH

HCl in the absence and the presence of MMH. Figure 6a represents the image obtained for polished MS without being exposed to the corrosive environment while Fig. 6b shows strongly damaged MS surface due to the formation of corrosion products after immersion in 1 M HCl. FESEM images of MS surface after immersion in 1 M HCl with 0.6 (g/L) MMH are shown in Fig. 6c. It is clear from the above figures that the protective film formation by the inhibitor on the MS surface protects it from corrosion. The EDS images of the MS specimen obtained after experiments with uninhibited and inhibited acids are given in Fig. 7a, b respectively. Analysis of Fig. 7a shows the presence of Fe, O, C signals. Whereas the surface of inhibited sample Fig. 7b shows the presence of Fe, O, Mn, C, Cl signals. Further, there is a decrease in the percentage of Fe in the inhibited MS surface. This confirms the adsorption of MMH extract molecule (Table 8) on the MS surface.

3.7 Fourier Transform Infrared Spectroscopy (FTIR)

FTIR spectroscopy is used to determine the functional groups present in the plant extract and examine the film adsorbed on a metal surface in protection against corrosion. Figure 8a shows the spectrum of the solid residue of MMH. A broad peak is obtained at 3309.2 cm^{-1} which

Table 8 EDS analysis results of Fresh MS of MS in 1 M HCl in the absence and presence of MMH

HCl medium	Composition (%)					
	Fe	Cl	C	O	Mn	Si
MS in 1 M HCl	61.25	–	5.79	32.96	–	–
MS in 1 M HCl + MMH	42.07	2.59	11.03	42.07	0.30	–

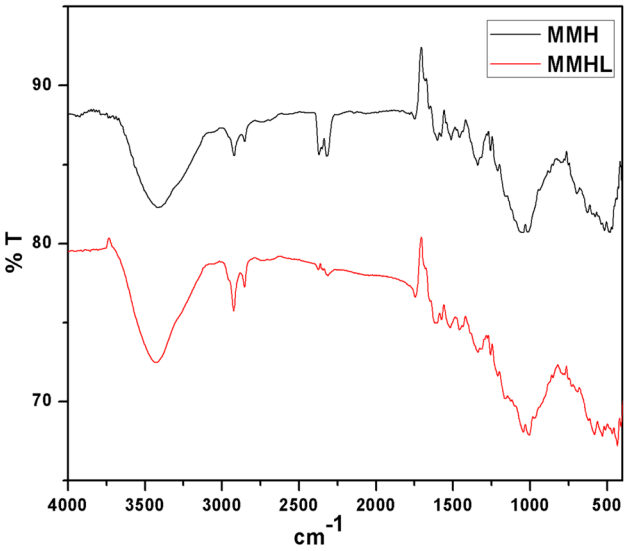

Fig. 8 FT-IR spectrum of MMH (**a**) and the scrapped material (**b**)

is assigned to OH or NH stretching vibration. The sharp peak at 2923.56 and 2852.2 cm^{-1} indicates the presence of $–CH_2$ asymmetrical stretching vibration. Peaks at 1687.41 and 1613.16 cm^{-1} are attributed to C=O and C=N stretching. The band at 1045.23 cm^{-1} is due to C–O stretching vibration. Further, the C–S stretching vibration was observed at 667.2 cm^{-1}. Comparison of Fig. 8b with a shows that the peak at 3309 cm^{-1} is shifted 3418 cm^{-1} and $–CH_2$ asymmetric stretching vibrations has shifted from 2923.5 to 2920.6 cm^{-1}. The absorption band at 1045 cm^{-1} shifted to 1014 cm^{-1}. The prominent bands at 515 cm^{-1}, 486 cm^{-1} are characteristic of Iron oxide. Figure 8b clearly shows the shift in frequencies of various functional groups indicating the adsorption of these chemical constituents on MS surface.

3.8 Comparison Studies

The comparisons of the results in Table 9 clearly indicate that the same trend in the performance of the inhibitor is noticed from the results obtained from all the techniques. However, the change in the numerical value of the percentage inhibition efficiency is due to the fact that the weight loss studies give average corrosion rate and the results from electrochemical studies give instantaneous corrosion rate. Further, the colorimetric studies evaluate the performance of the inhibitor from the amount of iron present in the solution after immersion studies i.e. after the corrosion process is over.

4 Conclusion

The methanol extract of MH leaves inhibits corrosion of MS in 1 M HCl. The inhibitor shows maximum efficiency with a 3-h immersion period. Increasing concentration of inhibitor increases the inhibition efficiency and the efficiency decreased while increasing the concentrations of acid. The addition of KBr produced a synergistic effect and the antagonistic effect is observed with KI addition. The inhibition efficiency of MMH decreases with increase in temperature, which suggests the adsorption process following physical adsorption mechanism. The adsorption of the extract followed a Langmuir adsorption isotherm. Polarization studies indicate that the MMH inhibitor acts as a mixed type inhibitor. The inhibition efficiency values obtained from weight

Table 9 Comparison of the results from different techniques

S. no.	MMH conc. (g/L)	%IE							
		Weight loss method			Colorimetric method			Electrochemical method	
		1 h	3 h	5 h	1 h	3 h	5 h	PDP	EIS
1	0.1	37.11	47.67	52.12	21.03	35.22	17.19	35.45	40.34
2	0.2	58.39	70.92	66.84	35.17	47.67	30.08	60.41	67.67
3	0.3	70.31	76.75	77.03	42.06	59.34	55.85	71.88	77.61
4	0.4	78.91	83.40	83.30	63.40	67.32	60.28	77.07	82.29
5	0.5	86.13	89.42	88.66	70.06	83.07	64.51	80.60	84.96
6	0.6	89.06	90.61	88.72	84.10	91.03	84.64	84.13	88.81

loss, colorimetric and electrochemical experiments are in good agreement. FESEM studies reveal the formation of a smooth surface on mild steel in the presence of MMH which indicates the formation of a good protective layer on the MS surface.

References

1. Verma DK, Khan F (2016) Corrosion inhibition of mild steel in hydrochloric acid using extract of glycine max leaves. Res Chem Intermed 42(4):3489–3506
2. Moretti G, Guidi F, Fabris F (2013) Corrosion inhibition of the mild steel in 0.5 M HCl by 2-butyl-hexahydropyrrolo [1,2-b][1,2] oxazole. Corros Sci 76:206–218
3. Raja PB, Qureshi AK, Rahim AA, Osman H, Awang K (2013) Neolamarckia cadamba alkaloids as eco-friendly corrosion inhibitors for mild steel in 1 M HCl media. Corros Sci 69:292–301
4. Ansari KR, Quraishi MA (2014) Bis-Schiff bases of isatin as new and environmentally benign corrosion inhibitor for mild steel. J Ind Eng Chem 20(5):2819–2829
5. Fouda AS, Abdallah M, Ahmed IS, Eissa M (2012) Corrosion inhibition of aluminum in 1 M H_3PO_4 solutions by ethanolamines. Arab J Chem 5(3):297–307
6. Deng S, Li X (2012) Inhibition by Jasminum nudiflorum Lindl. leaves extract of the corrosion of aluminium in HCl solution. Corros Sci 64:253–262
7. Zapata-Loría AD, Pech-Canul MA (2014) Corrosion inhibition of aluminum in 0.1 M HCL solution by glutamic acid. Chem Eng Commun 201(7):855–869
8. Markhali BP, Naderi R, Mahdavian M, Sayebani M, Arman SY (2013) Electrochemical impedance spectroscopy and electrochemical noise measurements as tools to evaluate corrosion inhibition of azole compounds on stainless steel in acidic media. Corros Sci 75:269–279
9. Hashim NM, Rahim AA, Osman H, Raja PB (2012) Quinazolinone compounds as corrosion inhibitors for mild steel in sulfuric acid medium. Chem Eng Commun 199(6):751–766
10. Li X, Deng S (2012) Inhibition effect of Dendrocalamus brandisii leaves extract on aluminum in HCl, H_3PO_4 solutions. Corros Sci 65:299–308
11. Krishnaveni K, Ravichandran J, Selvaraj A (2014) Inhibition of mild steel corrosion by *Morinda tinctoria* leaves extract in sulphuric acid medium. Ionics 20(1):115–126
12. Abdallah M, Al Karanee SO, Abdel AA, Fatah (2010) Inhibition of acidic and pitting corrosion of nickel using natural black cumin oil. Chem Eng Commun 197(12):1446–1454
13. Patel NS, Jauhari S, Mehta GN (2009) Mild steel corrosion inhibition by Bauhinia purpurea leaves extract in 1 N sulphuric acid. Arab J Sci Eng 34(2):61
14. Ramde T, Rossi S, Zanella C (2014) Inhibition of the Cu65/Zn35 brass corrosion by natural extract of *Camellia sinensis*. Appl Surf Sci 307:209–216
15. Fiori-Bimbi MV, Alvarez PE, Vaca H, Gervasi CA (2015) Corrosion inhibition of mild steel in HCL solution by pectin. Corros Sci 92:192–199
16. Shah AM, Rahim AA, Hamid SA, Yahya S (2013) Green inhibitors for copper corrosion by mangrove tannin. Int J Electrochem Sci 8(2):2140–2153
17. Dasami PM, Parameswari K, Chitra S (2015) Corrosion inhibition of mild steel in 1 M H_2SO_4 by thiadiazole Schiff bases. Measurement 69:195–201
18. Salghi R, Anejjar A, Benali O, Al-Deyab SS, Zarrouk A, Jama C, Hammouti B (2014) Inhibition effect of thymelaea hirsuta extract towards steel corrosion in HCl solution. Int J Electrochem Sci 9:5315–5327
19. Anupama KK, Abraham J (2013) Electroanalytical studies on the corrosion inhibition behavior of guava (*Psidium guajava*) leaves extract on mild steel in hydrochloric acid. Res Chem Intermed 39(9):4067–4080
20. Vimala J, Rosaline A, Leema Rose, Raja S (2011) *Cassia auriculata* extract as corrosion inhibitor for mild steel in acid medium. Int J ChemTech Res 3(4):1791–1801
21. Jyothi S, Ravichandran J (2014) *Luffa aegyptiaca* leaves extract as corrosion inhibitor for mild steel in hydrochloric acid medium. J Adhes Sci Technol 28(22–23):2347–2363
22. Mayakrishnan G, Pitchai S, Raman K, Vincent AR, Nagarajan S (2011) Inhibitive action of *Clematis gouriana* extract on the corrosion of mild steel in acidic medium. Ionics 17(9):843–852
23. Okafor PC, Euwah Ikpi M, Uwah IE, Ebenso EE, Ekpe UJ, Umoren SA (2008) Inhibitory action of *Phyllanthus amarus* extracts on the corrosion of mild steel in acidic media. Corros Sci 50(8):2310–2317
24. Hussin MH, Jain M, Kassim (2011) The corrosion inhibition and adsorption behavior of *Uncaria gambir* extract on mild steel in 1 M HCl. Mater Chem Phys 125(3):461–468
25. Quraishi MA, Singh A, Singh VK, Yadav DK, Singh AK (2010) Green approach to corrosion inhibition of mild steel in hydrochloric acid and sulphuric acid solutions by the extract of *Murraya koenigii* leaves. Mater Chem Phys 122(1):114–122
26. Gerengi H, Sahin HI (2011) *Schinopsis lorentzii* extract as a green corrosion inhibitor for low carbon steel in 1 M HCl solution. Ind Eng Chem Res 51(2):780–787
27. Gopiraman M, Sakunthala P, Kesavan D, Alexramani V, Kim IS, Sulochana N (2012) An investigation of mild carbon steel corrosion inhibition in hydrochloric acid medium by environment friendly green inhibitors. J Coat Technol Res 9(1):15–26
28. Kathiravan S, Ragul R, Raja G, Ravichandran J (2018) Theoretical and experimental studies about the inhibitive action of *Ruellia tuberosa* L. on mild steel in HCl medium. J Bio Tribo Corros 4(3):46
29. Sakunthala P, Vivekananthan SS, Gopiraman M, Sulochana N, Vincent AR (2013) Spectroscopic investigations of physicochemical interactions on mild steel in an acidic medium by environmentally friendly green inhibitors. J Surfactants Deterg 16(2):251–263
30. Chauhan LR, Gunasekaran G (2007) Corrosion inhibition of mild steel by plant extract in dilute HCl medium. Corros Sci 49(3):1143–1161
31. Idris ML, Nkafamiya II, Akinterinwa A, Japari JI (2015) Preliminary studies on some medicinal plants in Girei, Adamawa State of Nigeria. Br J Pharm Res 6(3):203–213
32. Jyothi S, Ravichandran J (2015) Inhibitive action of the acid extract of Luffa aegyptiaca leaves on the corrosion of mild steel in acidic medium. J Adhes Sci Technol 29(3):207–231
33. Jyothi S, Ravichandran J (2014) Corrosion inhibition of mild steel in sulphuric acid using Luffa Aegyptiaca leaves extract. Acta Metall Sin 27(6):969–980
34. Omo-Odudu DU, Oforka NC (1999) Inhibition of the corrosion of mild steel in trioxonitrate (v) acid Nig J Phys 11:148–153
35. Oguzie EE (2006) Adsorption and corrosion inhibitive properties of Azadirachta indica in acid solutions. Pigm Resin Technol 35(6):334–340
36. Oguzie EE, Onuchukwu AI, Okafor PC, Ebenso EE (2006) Corrosion inhibition and adsorption behaviour of *Ocimum basilicum* extract on aluminium. Pigm Resin Technol 35(2):63–70
37. Eddy NO, Odoemelam SA, Odiongenyi AO (2009) Joint effect of halides and ethanol extract of *Lasianthera africana* on

inhibition of corrosion of mild steel in H_2SO_4. J Appl Electrochem 39(6):849–857
38. Wu YC, Zhang P, Pickering HW, Allara DL (1993) Effect of KI on improving copper corrosion inhibition efficiency of benzotriazole in sulfuric acid electrolytes. J Electrochem Soc 140(10):2791–2800
39. Umoren SA, Solomon MM, Udosoro II, Udoh AP (2010) Synergistic and antagonistic effects between halide ions and carboxymethyl cellulose for the corrosion inhibition of mild steel in sulphuric acid solution. Cellulose 17(3):635–648
40. Shukla SK (2011) and E. E. Ebenso. Corrosion inhibition, adsorption behavior and thermodynamic properties of streptomycin on mild steel in hydrochloric acid medium. Int J Electrochem Sci 6(8):3277–3291
41. Singh A, Ahamad I, Singh VK, Quraishi MA (2011) Inhibition effect of environmentally benign Karanj (*Pongamia pinnata*) seed extract on corrosion of mild steel in hydrochloric acid solution. J Solid State Electrochem 15(6):1087–1097
42. Krishnaveni K, Ravichandran J (2014) Influence of aqueous extract of leaves of Morinda tinctoria on copper corrosion in HCl medium. J Electroanal Chem 735:24–31
43. Szauer T, Brandt A (1983) Equilibria in solutions of amines and fatty acids with relevance to the corrosion inhibition of iron. Corros Sci 23(12):1247–1257
44. Khaled KF (2003) The inhibition of benzimidazole derivatives on corrosion of iron in 1 M HCl solutions. Electrochim Acta 48(17):2493–2503
45. McCafferty E, Hackerman N (1972) Double layer capacitance of iron and corrosion inhibition with polymethylene diamines. J Electrochem Soc 119(2):146–154
46. Raja PB, Sethuraman MG (2008) Natural products as corrosion inhibitor for metals in corrosive media—a review. Mater Lett 62(1):113–116
47. Gunasekaran G, Chauhan LR (2004) Eco friendly inhibitor for corrosion inhibition of mild steel in phosphoric acid medium. *Electrochimica Acta, 49*(25), 4387–4395